

Structure of the blue phases of cholesteric liquid crystals

V. A. Kizel' and V. V. Prokhorov

Physicotechnical Institute, Moscow

(Submitted 2 February 1984)

Zh. Eksp. Teor. Fiz. **87**, 450-466 (August 1984)

The circular-dichroism spectra are measured for the three blue phases in a series of mixtures of cholesteryl nonanoate and cholesteryl chloride at normal and oblique incidence of the light. It is shown that the symmetry space groups are O^8 in the first phase and O^2 in the second phase. All of the possible discrete orientations of the cubic cell in the samples are determined in relation to the temperature, thermal history, and boundary conditions. The unit cell of the low-temperature blue phase is found to deform on supercooling. The circular-dichroism spectra are obtained for the third blue phase, which arises for small values of the cholesteric pitch. The data on the integrated intensity of the reflections are used to estimate the amplitudes of the Fourier components of the permittivity tensors of the first and second blue phases.

The so-called "blue phases" of chiral liquid crystals are currently of great interest both in connection with their interesting structural properties and from the standpoint of the general theory of phase transitions. In the past few years some progress has been made in the study of these phases both in their theoretical¹⁻³ and experimental⁴⁻⁸ aspects. It has been established experimentally that there are two or three thermodynamically stable blue phases in a narrow temperature interval between the cholesteric and isotropic phases of chiral liquid-crystalline materials for values of the cholesteric pitch that are not too large.⁴ Studies of the spectrophotometric and polarizational properties have established^{5,6} that the first two blue phases have a three-dimensional cubic chiral structure with cell dimensions of the order of the pitch of the cholesteric helix.¹ In Ref. 7 an attempt was made to estimate the ratio of the order parameters in the cholesteric and blue phases, but the experimental information is still extremely scanty and occasionally contradictory. Among the optical techniques a very informative method is to study the circular dichroism; this method has significant advantages over conventional reflection and transmission measurements for studying chiral objects. In

the present paper we utilize measurements of the circular dichroism to study the structures of the blue phases.

1. EXPERIMENTAL TECHNIQUES

The measurements were made on a Jobin Yvon Mark III dichrograph. The liquid crystal under study was placed between quartz plates, 20×20 mm in size, whose surfaces had been polished to $1/2$ fringe. The spacer thicknesses used were 3, 6, 12, and $25 \mu\text{m}$; the diameter of the investigated region was approximately 4 mm. A surface of the plates was covered by a thin layer of polyvinyl alcohol. After the film had polymerized, the surface was rubbed in a definite direction to produce an orienting effect. The quality of the resulting blue-phase textures was monitored in a special polarizing microscope both during the preparation of the sample and during the measurements. For each material (or mixture) studied, several (3-5 on the average) samples were prepared, from which we selected the most homogeneous. Complete homogeneity, however, even for the most careful preparation, was nearly impossible to achieve. The inhomogeneities are due, as a rule, to imperceptible defects in the coating (and the rubbing), since they arise at the same points in the sample

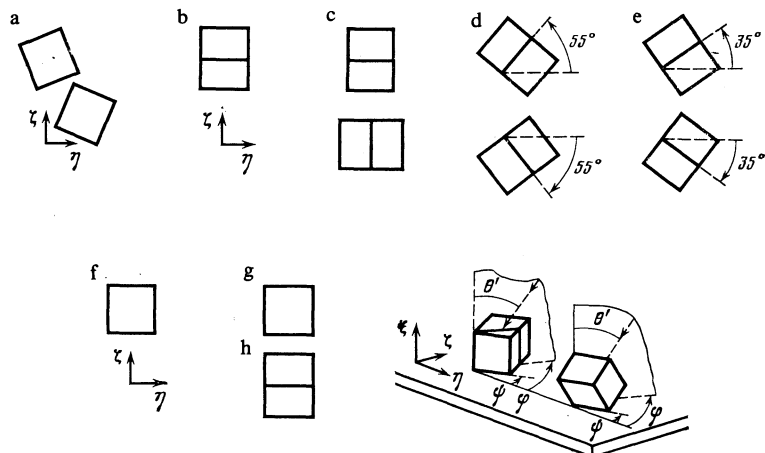


FIG. 1. Geometry of the measurements and the possible orientations of the unit cells in the samples: a) BP-I, heating from the cholesteric phase, polydomain; b) BP-I, cooling from BP-II, single-domain ($\psi = 0^\circ$); c) the same, polydomain (upper $\psi = 0^\circ$, lower $\psi = 90^\circ$); d) the same ($\psi = \pm 55^\circ$); e) the same ($\psi = \pm 35^\circ$); f) BP-II, single-domain ($\psi = 0^\circ$); g) BP-II, polydomain ($\psi = 0^\circ$); h) the same ($\psi = 90^\circ$). The diagrams show the projections of the cubic cell onto the surface; η is the direction of the orientational rubbing.

at all the transitions, both forward and backward.²⁾ Consequently, the transitions between phases at different points in the sample occur at somewhat different (by hundredths of a degree) temperatures, and within a given phase in the sample there are separate, extremely small "domains" with a different orientation (see below) of the blue-phase structure.

The temperature-regulating system maintained the temperature to better than $\pm 0.005^\circ\text{C}$.

The angle of incidence θ and the azimuth φ of the direction in which the substrate was rubbed (measured with respect to the plane of incidence; Fig. 1) could be adjusted arbitrarily by rotating the oven and sample as a whole; this is important in determining the azimuthal orientation of the blue-phase structures in the sample. The samples were held at a fixed temperature for 30–40 min before the measurements were made; in a number of cases, in order to obtain a single-domain structure (primarily for BP-1), the samples were held at a fixed temperature for several hours.

Measurements were made in acenic esters of cholesterol, their binary mixtures, and several other chiral materials. The most detailed studies were done for mixtures of cholesteryl nonanoate (CN) and cholesteryl chloride (CC), which are dextrorotatory and levorotatory, respectively. The appreciable fundamental absorption of these compounds lies in the region $\lambda \leq 220\text{ nm}$. The materials used had been subjected to a chromatographic purification. As we show below, the general behavior of all the materials studied is qualitatively similar and depends importantly only on pitch of the cholesteric helix. Therefore, in this report we shall discuss only the results for the mixtures indicated above.

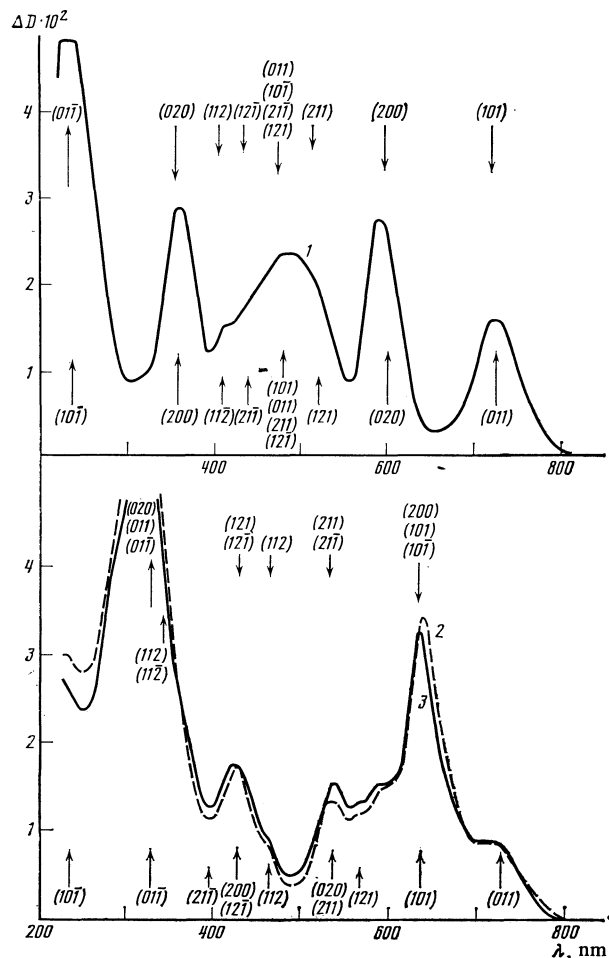


FIG. 2. Circular-dichroism spectrum of the 65:35 mixture; sample thickness $12\ \mu\text{m}$, BP-I, cooling from the isotropic phase, $T = 77.65^\circ\text{C}$, $\theta = 27^\circ$, polydomain sample: 1) $\varphi = 0^\circ$, 2) $\varphi = 35^\circ$, 3) $\varphi = -35^\circ$. The lower and upper arrows indicate the positions of the reflections for the domains with $\psi = 55^\circ$ and $\psi = -55^\circ$, respectively. The arrows in the lower figure refer to curve 2.

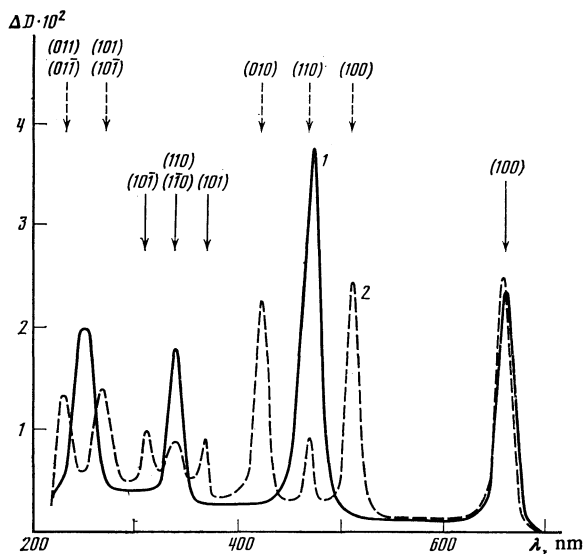


FIG. 3. Circular-dichroism spectrum of the 73:27 mixture; sample thickness $6\ \mu\text{m}$, BP-II, cooling from the isotropic phase, $T = 76.60^\circ\text{C}$, polydomain sample: 1) $\theta = 0^\circ$, $\varphi = 90^\circ$; 2) $\theta = 8^\circ$, $\varphi = 90^\circ$. The solid and dashed arrows indicate the positions of the reflections for the BP-II domains oriented as in Fig. 1g and 1h, respectively.

teryl nonanoate (CN) and cholesteryl chloride (CC), which are dextrorotatory and levorotatory, respectively. The appreciable fundamental absorption of these compounds lies in the region $\lambda \leq 220\text{ nm}$. The materials used had been subjected to a chromatographic purification. As we show below, the general behavior of all the materials studied is qualitatively similar and depends importantly only on pitch of the cholesteric helix. Therefore, in this report we shall discuss only the results for the mixtures indicated above.

2. GENERAL PICTURE

In Figs. 2–9 we present the most typical of the circular-dichroism (ΔD) spectra obtained in this study, for mixtures

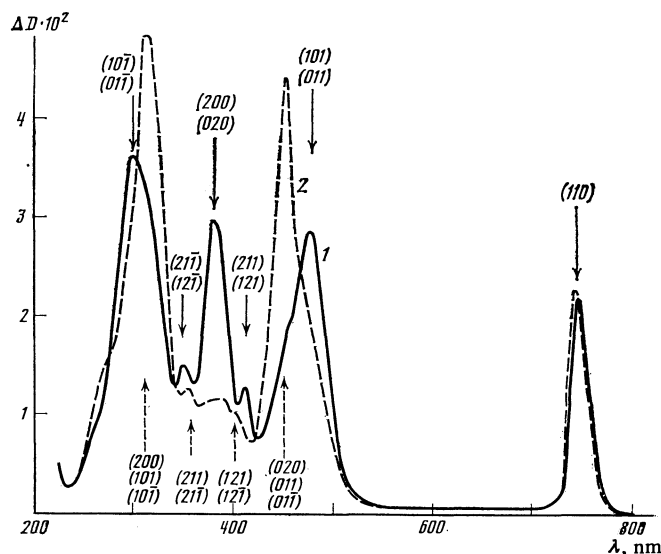


FIG. 4. The same as in Fig. 3, but for BP-I in cooling from BP-II, $T = 76.50^\circ\text{C}$, single-domain sample, $\theta = 15^\circ$: 1) $\varphi = 0^\circ$; 2) $\varphi = 90^\circ$.

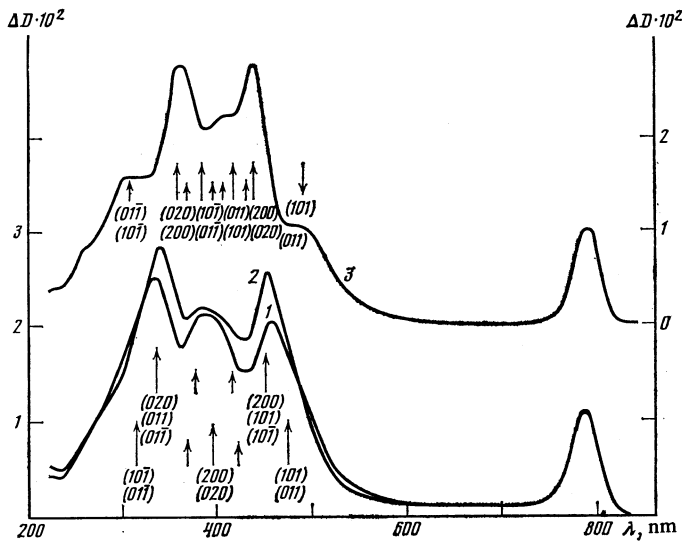


FIG. 5. The same as in Fig. 4, but for $T = 76.49^\circ\text{C}$, polydomain sample, $\theta = 12^\circ$: 1) $\varphi = 0^\circ$; 2) $\varphi = 90^\circ$; 3) $\varphi = 45^\circ$. The upper and lower arrows indicate the positions of the reflections for the domains with $\psi = 90^\circ$ and $\psi = 0^\circ$ (curve 2), respectively. The short arrows all indicate the positions of the (211) , $(21\bar{1})$, (121) , and $(12\bar{1})$ reflections.

of CN and CC in different ratios and for different samples of the same mixture.

Let us first discuss the general features common to all the mixtures in the normal-incidence spectra.

All of the phases give a series of chiral reflections and, accordingly, peaks in the circular dichroism. The spectral position of the reflections³⁾ is governed mainly by the pitch of the cholesteric helix in the cholesteric phase of the mixture and is practically independent of the composition. At selective-reflection wavelengths λ_{sr} greater than about 800 nm there were no blue phases at all in the mixtures. As the helical pitch decreased, the phase BP-I appeared first, and as the pitch decreased further a second (high-temperature) phase, BP-II, also appeared, existing in mixtures with $\lambda_{sr} \leq 700$ nm. In mixtures with $\lambda_{sr} \leq 450$ nm there is still another phase (between BP-II and the isotropic phase), which has been dubbed BP-III in the literature; this phase does not give narrow spectral reflections like those which are typical of BP-I and BP-II. The reflections of the first two phases are strictly and reproducibly localized in frequency, and their wave-

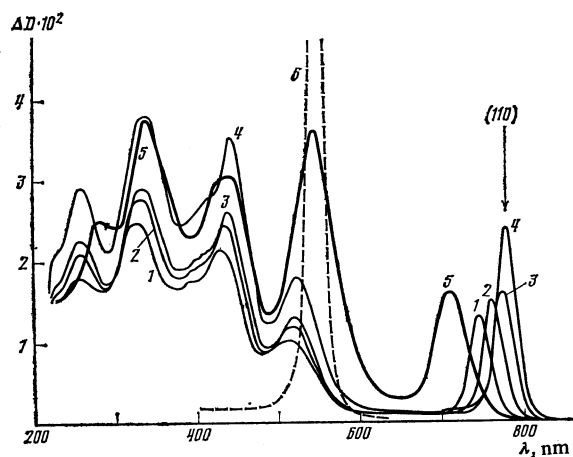


FIG. 6. The same as in Fig. 5 but for $\theta = 18^\circ$ and $\varphi = 35^\circ$, at various temperatures: 1) 76.42°C ; 2) 76.36°C ; 3) 76.58°C ; 4) 75.80°C ; 5) 75.45°C ; 6) 75.30°C (the transition to the cholesteric phase).

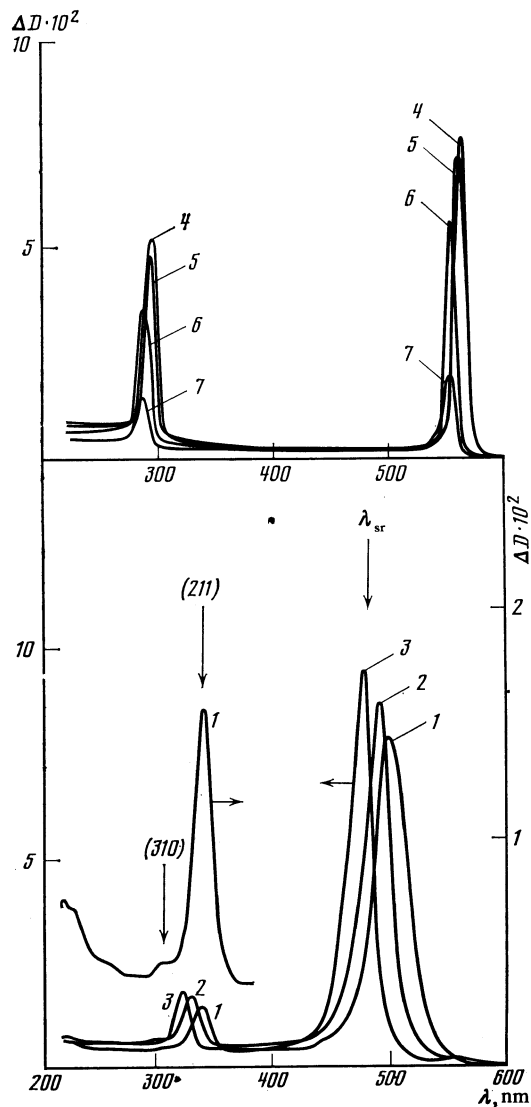


FIG. 7. Circular-dichroism spectrum of the 80:20 mixture, sample thickness $6\ \mu\text{m}$, heating from the cholesteric phase, $\theta = 0^\circ$. BP-I at various temperatures: 1) 83.55°C , 2) 83.60°C , 3) 83.65°C ; BP-II: 4) 83.68°C , 5) 83.70°C , 6) 83.72°C , 7) 83.74°C .

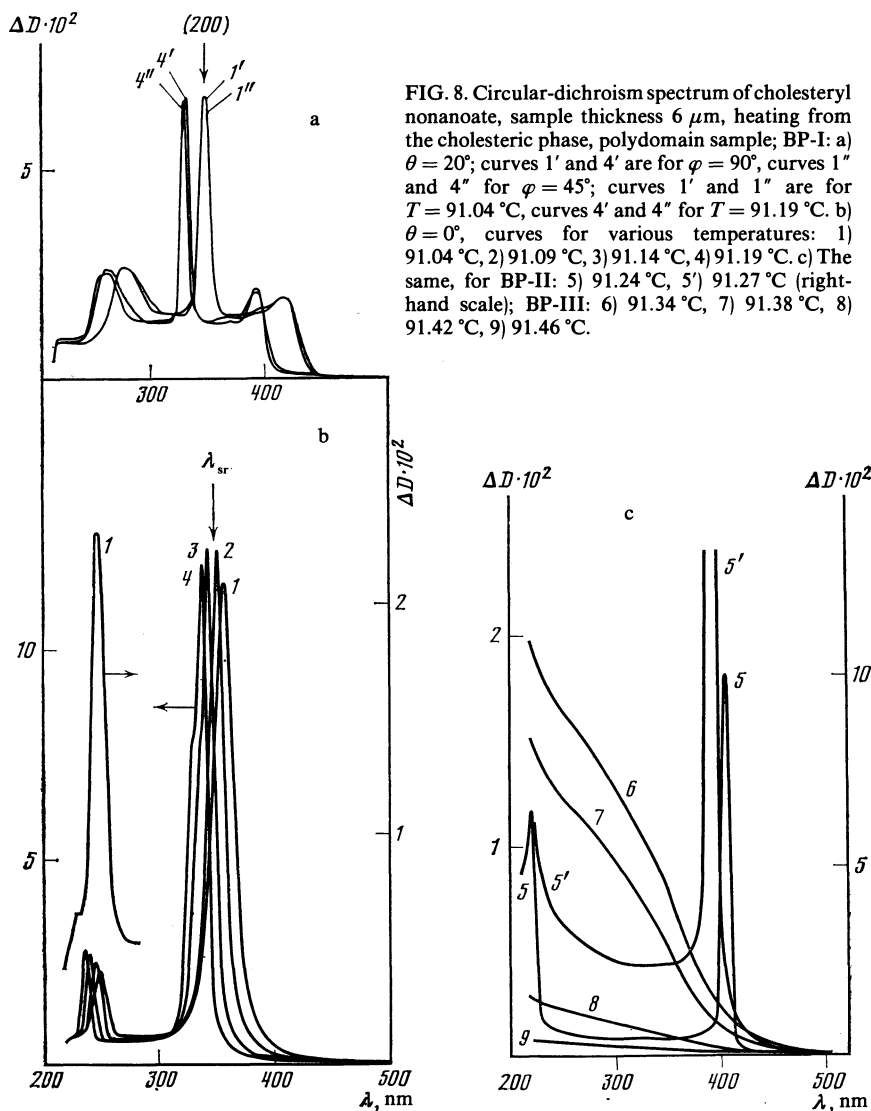


FIG. 8. Circular-dichroism spectrum of cholesteryl nonanoate, sample thickness $6 \mu\text{m}$, heating from the cholesteric phase, polydomain sample; BP-I: a) $\theta = 20^\circ$; curves 1' and 4' are for $\varphi = 90^\circ$, curves 1'' and 4'' for $\varphi = 45^\circ$; curves 1' and 1'' are for $T = 91.04^\circ\text{C}$, curves 4' and 4'' for $T = 91.19^\circ\text{C}$. b) $\theta = 0^\circ$, curves for various temperatures: 1) 91.04°C , 2) 91.09°C , 3) 91.14°C , 4) 91.19°C . c) The same, for BP-II: 5) 91.24°C , 5') 91.27°C (right-hand scale); BP-III: 6) 91.34°C , 7) 91.38°C , 8) 91.42°C , 9) 91.46°C .

lengths are related to one another by small integers (if one allows for the dispersion of the refractive index.⁴⁾ Furthermore, the pattern of circular dichroism (primarily for the low-temperature phase BP-I) depends on the thermal history. The spectrum of BP-I for different materials and mixtures exhibits three strong reflections (the weaker reflections will be discussed further on), with wavelengths in the ratio

$$\lambda_1^a : \lambda_2^a : \lambda_3^a = 1 : 2/3 : 1/3$$

for the BP-I phase obtained by heating from the cholesteric phase, and in the ratio

$$\lambda_1^c : \lambda_2^c : \lambda_3^c = 1 : 1/2 : 1/3$$

for the BP-I phase obtained by cooling from BP-II; here $\lambda_1^H : \lambda_1^C = 1 : \sqrt{2}$ (the third, short-wavelength reflection usually lies in the fundamental absorption region and is seen only in mixtures having a long enough cholesteric pitch).

In contrast to the case of BP-I, the circular-dichroism spectrum of the high-temperature phase BP-II depends very little on the thermal history. At normal incidence one observes either two reflections with a wavelength ratio

$\lambda_1 : \lambda_2 = 1 : 1/2$ or else these two reflections plus another pair, having the same wavelength ratio $\lambda_1' : \lambda_2' = 1 : 1/2$ but shifted to shorter wavelengths by a factor $\lambda_1' : \lambda_1 = 1/\sqrt{2}$. Polarimetric observations show that in the first case the sample is uniformly colored and, as we shall see below, in a single-domain state, while in the second case there are regions of different color and, accordingly, different orientation.

The results were interpreted using a technique which we have described previously.⁸ We considered two possible blue-phase structures—simple cubic and body-centered cubic—and a number of physically plausible alternative orientations of the unit cell in the sample; the spectral position of the reflections was calculated for each of the alternatives. The choice is completely unambiguous, since the different alternatives give qualitatively different patterns for the circular dichroism.

Let us explain the calculational technique in some detail. Since we have $\lambda_1^H : \lambda_1^C = 1/\sqrt{2} = \cos 45^\circ$ for BP-I and $\lambda_1' : \lambda_1 = \cos 45^\circ$ for BP-II, it is logical to suppose that the cubic cells in the different domains are rotated by an angle of 45° with respect to each other and that the normal to the surface

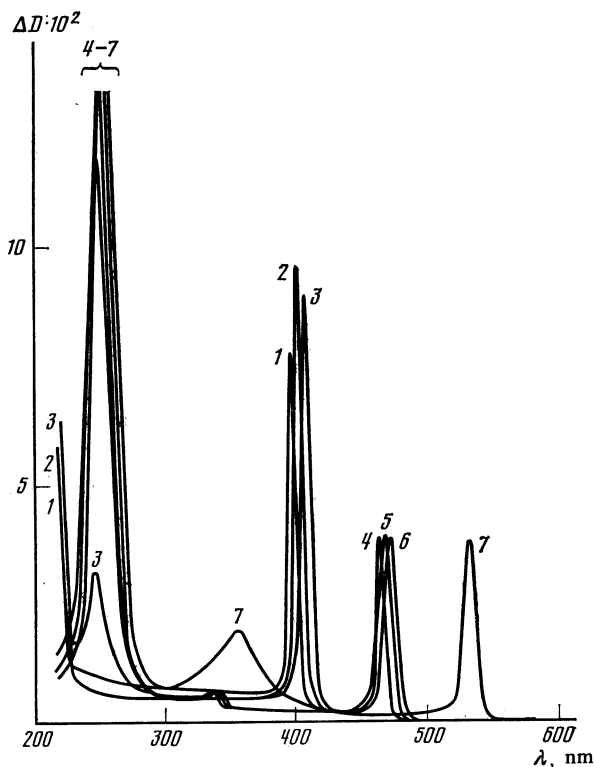


FIG. 9. The same as in Fig. 8, for cooling from the isotropic phase, $\theta = 0^\circ$, various temperatures; BP-II: 1) 91.22 °C, 2) 91.02 °C, 3) 91.17 °C; BP-I: 4) 91.12 °C, 5) 91.07 °C, 6) 91.02 °C, 7) 90.45 °C.

is in the [100] direction in one case and in the [110] direction in the other. As we shall see, these assumptions bear a good resemblance to the actual situation. One easily obtains the following two relations for the wavelength of the reflection

with Miller indices hkl at these two orientations of the cell (the scattering geometry and choice of coordinate axes are indicated in Fig. 1):

$$\lambda_{hkl} = 2(h^2 + k^2 + l^2)^{-1} [h \cos \theta' + k \sin \theta' \cos \varphi' + l \sin \theta' \sin \varphi'] na,$$

$$\lambda_{hkl} = \sqrt{2}(h^2 + k^2 + l^2)^{-1} [(h+k) \cos \theta' + (h-k) \sin \theta' \cos \varphi' + \sqrt{2}l \sin \theta' \sin \varphi'] na; \quad (1)$$

here $\varphi' = \varphi - \psi$, a is the dimension of the unit cell, n is the average refractive index, θ' is the angle of incidence in the blue phase ($\sin \theta' = n^{-1} \sin \theta$, where θ is the angle of incidence on the sample, reckoned from the normal to its surface—the ξ axis), φ is the azimuth of the plane of incidence with respect to the η axis, which coincides with the direction in which the substrate was rubbed, ψ is the angle between the η axis and the [010] direction of the blue phase in the first case and the [001] direction in the second case. The angles φ and ψ are measured counterclockwise from the η axis.

Table I gives the relative wavelengths of the first 12 reflections as calculated by formulas (1) in the case of normal incidence for the two cell orientations indicated above and for an orientation in which the normal to the surface is in the [111] direction. It is seen that for BP-I there is agreement with experiment only for the assumption of a body-centered cell and only for two orientations of this cell: In the BP-I phase obtained by heating from the cholesteric phase, the normal to the surface is in the [100] direction, while in the phase obtained by cooling the normal is in the [110] direction. The hypothesis that the (100) reflection of the simple cubic lattice could be present but located in the infrared region for certain mixtures is ruled out for BP-I by the data for the mixtures with the smallest cell dimensions.

TABLE I. Relative wavelengths of the circular-dichroic reflections at normal incidence.

hkl	λ_{hkl}	$\lambda_{hkl} : \sqrt{2}$	$\lambda_{hkl} : \sqrt{4/a}$
100	2	1	1
110 X	1	1, 1/2	1
111	2/3	2/3	1, 1/3
200 X	1	1/2	1/2
210	4/5, 2/5	3/5, 2/5	3/5, 1/5
211 X	2/3, 1/3	1/2, 1/3	2/3, 1/3
220 X	1/2	1/2, 1/4	1/2
221	4/9, 2/9	4/9, 3/9	5/9, 3/9, 1/9
222 X	1/3	1/3	1/2, 1/6
310 X	3/5, 1/5	4/10, 3/10	4/10, 2/10
320	6/13, 4/13	5/13, 3/13, 2/13	5/13, 1/13
321 X	3/7, 2/7	5/14, 4/14, 3/14	6/14, 4/14, 2/14
411 X	4/9	5/18, 2/18	6/18, 4/18

Notes: 1) The second, third, and fourth columns of the table show the wavelengths of the circular-dichroic reflections for cell orientations [100], [110], [111], respectively. 2) Since at normal incidence the reflections as a rule are degenerate in frequency, the index hkl in the left-hand column corresponds to a number of reflections. For example, for the [100] orientation there are 4 reflections with a wavelength of $\frac{2}{3}$, viz., (211), (21 $\bar{1}$), (2 $\bar{1}1$), and (2 $\bar{1}\bar{1}$), which are abbreviated (2{11}), and 8 reflections of the same type with wavelength $\frac{1}{3}$, viz. (112), (11 $\bar{2}$), (1 $\bar{1}2$), (1 $\bar{1}\bar{2}$), (1 $\bar{2}1$), (12 $\bar{1}$), (12 $\bar{1}$), and (1 $\bar{2}\bar{1}$), abbreviated (1{21}), as is indicated in the table. For the cell orientation [110] there are 4 reflections with wavelength $\sqrt{2}/2$, viz., the (211), (21 $\bar{1}$), (121), and (12 $\bar{1}$) reflections, and 2 reflections with wavelength $\sqrt{2}/3$, viz., (112) and (11 $\bar{2}$). 3) The symbol X denotes reflections which are allowed in the body-centered lattice; in the simple cubic lattice all the reflections indicated in the table are allowed. 4) The (111) reflection for the simple cubic and the (222) reflection for the body-centered lattice are forbidden in the circular dichroism by reasons of symmetry (Refs. 2 and 3). 5) The reflections of orders 5 and higher usually lie outside the working range of the dichrograph and are not indicated in the table.

It is also seen from Table I that for positive identification of the reflections we need data for oblique incidence. In this case the degeneracy of the reflections is partially or completely lifted, and from the character of the splitting of the reflections one can determine simultaneously the azimuthal orientation of the blue-phase cells in the sample. The alternative cell orientations for BP-I established by analysis of the circular-dichroism spectra for oblique incidence are shown in Figs. 1a–1e. The assignments given to the reflections in the following figures were arrived at by comparing the measured positions of the maxima with the results calculated with formulas (1) under the aforementioned assumptions about the orientation. The calculated spectral positions of the reflection peaks are indicated by arrows in all the figures.

For BP-II a similar analysis shows that the cell is simple cubic, and only the (100) and (110) reflections are observed; the possible orientations are shown in Figs. 1f–1h.

3. ANALYSIS OF THE DATA FOR VARIOUS MIXTURES

Let us examine the details of the patterns for the various mixtures, arranging them in order of decreasing pitch. With each case as an example we shall demonstrate certain additional general regularities. Table II gives the measured positions of the reflections and their assignments for mixtures of CN and CC in the ratio of 65:35 mole percent (hereafter called simply 65:35). The cholesteric pitch here is close to the maximum value at which the transition from the cholesteric phase to the isotropic phase still goes through intermediate blue phases. In this case one observes only a single blue phase, identified by the character of the spectrum as BP-I; the spectral width of the reflections here is somewhat larger than for the mixtures with shorter pitches, apparently because of the lower degree of order. The temperature region in which the “pure” BP-I exists during heating⁵⁾ is relatively small here, amounting to about 0.03 °C. In this temperature interval the peak intensities of the circular-dichroic reflections remain roughly unchanged, while the peak itself is shifted to shorter wavelengths (corresponding to a smaller cell dimension a) with increasing temperature; similar behavior occurs in all the other mixtures (Table II). This observation is in agreement with Refs. 10 and 11. Upon a further increase in temperature inclusions of the isotropic phase appear, as is usual in melting, and the dimensions of these inclusions (of the order of tens of μm) gradually increase with

increasing temperature. The peaks in the circular-dichroism spectra here gradually decrease in height to zero (but now with no shift in wavelength), and the pattern remains unchanged during prolonged holds at constant temperature—apparently there is coexistence of the isotropic and BP-I phases here.

In a previous paper⁸ we reported obtaining a single-domain sample of BP-I in one of the mixtures by cooling from BP-II; the orientation of the unit cell was that shown in Fig. 1b. In the majority of the other samples, regardless of the mixture composition, the situation was more complex—the sample turned out to be polydomain, but the [110] direction in all the domains was normal to the surface of the substrate and only the azimuthal orientation of the cells with respect to the rubbing direction changed. Domains such as these cannot be distinguished by observations in polarized light, and their presence can be established only for the case of oblique incidence, by superposition of the characteristic circular-dichroism spectra for each of them.⁶⁾ It was found that various samples exhibit a discrete set of the alternative cell orientations of the BP-I phase obtained by cooling from BP-II or from the isotropic phase (Figs. 1b–1e).

Figure 2 shows the circular-dichroism spectra corresponding to one of these alternatives in a sample of the 65:35 mixture. The wavelength of the (110) reflection in this case is 950 nm and lies outside the sensitivity limits of the dichrograph. The circular-dichroism pattern for $\varphi = 0$ (curve 1) can be explained by assuming the presence of domains with the azimuthal orientations shown in Fig. 1d. Analysis of curves 2 and 3 shows that they in fact correspond to a superposition of the circular-dichroism spectra from domains of the two types shown in Fig. 1d, with the total areas of both domain types being approximately the same, since curves 2 and 3 are almost identical. It is seen that the spectral positions calculated for the reflections under these assumptions are in good agreement with the experimental positions. A study of the circular-dichroism spectra of the other samples of this and the other mixtures showed that in addition to the domains described above, with cell orientation $\psi = \pm 55^\circ$ (Fig. 1d), a certain fraction of the sample area could be occupied by domains with cell orientations $\psi = 0^\circ$ and $\psi = 90^\circ$ (Fig. 1c) and $\psi = \pm 35^\circ$ (Fig. 1e).

Figure 3 shows the circular-dichroism spectra obtained for a 73:27 mixture during cooling from the isotropic phase. For the BP-II phase at normal incidence (curve 1 in Fig. 3)

TABLE II. Spectral position and identification of the reflections in BP-I obtained by heating and in the cholesteric phase for several mixtures of cholesteryl nonanoate (CN) and cholesteryl chloride (CC) at normal incidence.

Mixture CN:CC	$\begin{pmatrix} 200 \\ 1\{10\} \end{pmatrix}$	$(2\{11\})$	$(1\{21\})$	$T, ^\circ\text{C}$
65 : 35	745	498	256	77,70
	737	490	253	77,73
80 : 20	498	339	1)	83,55
	473	321		83,65
100 : 0	359	249	1)	91,04
	337	235		91,16
10 : 90	479	327	1)	66,06
	472	323		66,12

Note: Reflections 1) lie outside the sensitivity range of the dichrograph ($\lambda < 200 \text{ nm}$).

there are 4 reflections with a wavelength ratio of approximately $1:1/\sqrt{2}:1/2:1/2\sqrt{2}$. The first and third occupy the same spectral positions that were described in Ref. 8 for the single-domain sample of BP-II; the oblique-incidence data imply that these reflections correspond to domains with the cell orientation shown in Fig. 1g. The second and fourth reflections correspond to domains with a different cell orientation, as shown in Fig. 1h. No other orientations of the BP-II cell were observed in any of the samples. In both cases only the (100) and (110) reflections contribute to the circular-dichroism spectra. The reflections (210) and (211), which are allowed by symmetry in all the possible space groups, should have appeared at wavelengths in the working region of the detector but were not observed.

Figure 4 shows the circular-dichroism spectrum of a BP-I sample with the predominant cell orientation shown in Fig. 1b. The weak circular-dichroism peak on curve 1 in the 380-nm region and the slight asymmetry of the wings of curves 1 and 2 are evidently due to a small admixture of embedded domains with cell orientation $\psi = 90^\circ$. In the BP-I phase of this mixture some of the samples also exhibited the alternative orientation of Fig. 1d, which was described above for the 65:35 mixture. In other samples we found predominantly the cell orientation shown in Fig. 1c. Figure 5 shows the circular-dichroism spectrum of the same samples at oblique incidence. The patterns for azimuthal angles $\varphi = 0^\circ$ and $\varphi = 90^\circ$ (curves 1 and 2) correspond in terms of the character of the spectrum to a superposition of the circular-dichroism patterns from domains oriented as shown in Fig. 1c; here, by virtue of the similarity of curves 1 and 2, the number of domains with $\psi = 0^\circ$ and $\psi = 90^\circ$ are approximately equal. The spectral positions of the reflections as calculated under this assumption for $\varphi = 45^\circ$ coincide with the experimental positions (curve 3).

Figure 6 shows a series of circular-dichroism spectra of supercooled BP-I for this same mixture, but in a different sample (cell orientation as shown in Fig. 1b). We note two interesting features:

1) It is seen that the circular-dichroic reflection (110) is shifted appreciably to longer wavelengths upon supercooling,⁷⁾ whereas all the other reflections remain practically in place [for normal incidence the wavelengths of the circular-dichroic reflections (101), (10 $\bar{1}$), (011), (01 $\bar{1}$), and (200), (020) coincide]. This behavior indicates a distortion of the cubic cell of BP-I and was observed in all the mixtures studied. As a straightforward calculation shows, this behavior corresponds to a cell deformation of the following nature: If the relative change in the [110] dimension is denoted by x , then with accuracy to terms of second order in x

$$a_{[110]} = \sqrt{2}a_0(1+x), \quad a_{[1\bar{1}0]} = \sqrt{2}a_0 = \text{const}, \quad (2)$$

$$a_{[002]} = a_{[200]} = a_{[020]} = a_0(1+x/2),$$

here $a_{[hkl]}$ is the dimension (period) in the $[hkl]$ direction, and a_0 is the [200] dimension of the undistorted cubic cell. The dimension in the [110] direction, parallel to the plane of the substrate at the given orientation of the BP-I cell, remains unchanged as the cell becomes strained. The values of the strain x are small here—as the temperature of BP-I is

lowered, the strain gradually increases from zero (the undistorted cell) to 0.05, while the frequency ratio $z = \nu_{\text{sh}}/\nu_{(110)} = n_{\text{sh}}\lambda_{(110)}/n_{(110)}\lambda_{\text{sh}}$ between the set of degenerate (at normal incidence) short-wavelength reflections and the (110) reflection changes from 2 to 2.10.

2) A more interesting feature is the abrupt change in the circular-dichroism spectra (curve 5 in Fig. 6) as the temperature is lowered further into the strong supercooling region of BP-I. At normal incidence (curves not shown) the short-wavelength reflections are degenerate here as well, but the ratio z in this case decreases to 1.87. The resulting texture is unstable and gradually converts to the cholesteric phase; a similar behavior was observed in all the mixtures, without exception, at a sufficiently high supercooling of BP-I, and the changes in texture during the abrupt rearrangement of the cell are clearly visible in polarized light. The structure of the blue-phase cell arising after the transition is difficult to determine unambiguously on account of its instability.

The data for an 80:20 mixture are shown in Fig. 7. In the region of the short-wavelength wing of the (211) reflection one can, at the higher sensitivity, clearly resolve the (310) reflection, whose observation in a 73:27 mixture was reported in Ref. 8. The (321) reflection reported in that paper is located in the present mixture at the edge of the absorption band, and at the given linewidths it should merge with the line of the (411) reflection, whose wavelength differs from that of the (321) peak by only a factor of 1.035. We see that the existence region of BP-I is approximately 0.1 °C wide, while the “pure” BP-II exists only in a 0.05–0.06 °C interval (curves 4 and 5). Spectra 6 and 7 correspond to the coexistence region of BP-II and the isotropic phase, in the sense described above for BP-I in the 65:35 mixture.

For another sample of the 80:20 mixture we measured the circular dichroism for the BP-I phase obtained by cooling from BP-II, for decreasing temperature and in the presence of supercooling; here also we observe a pattern analogous to that shown in Fig. 6, i.e., the (110) reflection at first shifts to longer wavelengths relative to the other reflections and then abruptly shifts to shorter wavelengths upon strong supercooling.

Let us now go to the case of pure CC, for which $\lambda_{\text{sr}} = 352$ nm. For pure CC the transition from the cholesteric to the isotropic phase takes place (Fig. 8) through three intermediate blue phases. The oblique-incidence circular-dichroism spectra for the BP-I phase obtained by heating from the cholesteric phase do not depend on the azimuthal angle (Fig. 8a, curves 1', 1'', 4', 4''); consequently, one can state that there is no preferred direction of azimuthal orientation for the BP-I cells (Fig. 1a). The (200) reflection is seen here against the background of a wide band consisting of four reflections which are degenerate at normal incidence: (110), (1 $\bar{1}0$), (101), and (10 $\bar{1}$).

The spectral line shape of this band is easily explained on the basis of the following considerations: It follows from (1) that the change in the azimuthal orientation ψ of the BP-I cell affects the spectral position of the corresponding reflection in first order in $\Delta\psi$ at the center of the band ($\Delta\lambda \sim \Delta\psi$) and only in second order ($\Delta\lambda \sim (\Delta\psi)^2$) at the edges. Therefore,

if the azimuthal orientation of the domains is arbitrary, the combined circular-dichroism contour of the above reflections at oblique incidence will have two asymmetric peaks at the edges and a monotonic decrease at the center. A similar pattern was observed for all the mixtures (see Ref. 8).

The existence region of BP-I in CN is about 0.15 °C in width, that of BP-II about 0.10 °C, and that of BP-III about 0.06 °C. We note here that for this mixture, as for all the others in the figures, the BP-II reflection peaks are shifted slightly to shorter-wavelengths as the temperature is raised; the shift is similar to that indicated in Table II for BP-I, but considerably smaller.

For the case of decreasing temperature, the patterns for BP-III and BP-II are repeated, but for BP-I, as in the other mixtures, the cells are oriented predominantly with their [110] direction normal to the bounding surface (Fig. 9).

The weak circular-dichroism peak in the 340-nm region on the curves in Fig. 9 is due to the presence of a small number of BP-I domains with the orientation shown in Fig. 1a. The distortion of the BP-I cells in CN upon supercooling is represented by curve 7. This curve corresponds to the maximum wavelength of the (110) reflection and a strain $\alpha = 0.1$. Upon further supercooling the opposite behavior is observed—the wavelength of the (110) reflection starts to decrease (curves not shown). A similar nonmonotonic behavior was also observed in the other mixtures with small unit-cell dimensions. As regards the abrupt structural rearrangement of BP-I discussed above (Fig. 6), here it occurs only at a high degree of supercooling, about 2 °C.

4. DETERMINATION OF THE FOURIER COMPONENTS OF THE PERMITTIVITY TENSOR

The data which we have obtained permit calculation of the relative values of the Fourier components of the permittivity tensor. The values of ϵ_{hkl} were determined from measurements of the relative integrated intensities I of the circular-dichroic reflections. Since the values of the circular dichroism for the sample thicknesses used in this study were not more than a few hundredths, we used in our analysis the formula for I obtained in the kinematic approximation to the theory developed in Ref. 3 for the optical properties of the

blue phases:

$$I_{hkl} \equiv \int \Delta D_{hkl}(\lambda) d\lambda \sim L \epsilon_{hkl}^2 \frac{1 + \sin^2 \theta_B^{hkl}}{\sin^2 \theta_B^{hkl}}, \quad (3)$$

where L is the sample thickness, $\Delta D(\lambda)$ is the circular dichroism, and θ_B^{hkl} is the Bragg angle. Formula (3) was obtained under the assumption that the expansion of the tensor ϵ_{hkl} in the structural modes contains only a single mode²; then ϵ_{hkl} in formula (3) is the amplitude of this mode (i.e., is the scalar coefficient in the expansion of ϵ in the unit tensors corresponding to the spatial spherical harmonics).

In Ref. 7 a method was proposed for determining ϵ from the half-width of the selective-reflection band under conditions such that the light of one of the polarizations is totally reflected. However, this method is suitable only for the strongest reflections and, above all, requires rather thick samples with a very high-quality blue phase texture. Our method is insensitive to deformations in the texture and yields values of all the ϵ 's to a higher accuracy.

In the method which we have proposed, the calculations are done under the assumption that in cases of degeneracy the integrated intensities of the reflections are additive. The results are given in Table III. The uncertainty of the measurements is mainly due to the difficulty in making accurate allowance for the background and for the wings of the circular-dichroism curves; the instrumental error is much smaller ($\sim 10^{-3}$). A few comments: For BP-I we used the data for normal and oblique incidence for the case of heating from the cholesteric phase. The data for oblique incidence enabled us to determine the ratio $\epsilon_{200}^I : \epsilon_{110}^I$, and then the value of ϵ_{211}^I was determined from the normal-incidence measurements. The accuracy here was relatively high, approximately 5%. The ratio $\epsilon_{200}^I : \epsilon_{110}^I$ could have been determined solely from the normal-incidence data by bringing in the circular-dichroism spectra of the BP-I phase obtained by cooling from BP-II (with cell orientation [110]), as was done in Ref. 8, but the accuracy would be lower because the error in the measurements of the integrated intensity of the short-wavelength reflection is more critical. The results for the BP-I phase of the first two mixtures are given for the extreme temperature points in the BP-I existence interval—the first

TABLE III. Relative values of the Fourier components of the permittivity tensor of BP-I and BP-II in mixtures of cholesteryl nonanoate and cholesteryl chloride.

Mixture CN:CC	λ_{sr} , nm	$\epsilon_{200}^I : \epsilon_{110}^I : \epsilon_{211}^I$	$T_{BP-I, c}$	$\epsilon_{100}^{II} : \epsilon_{110}^I$	$\epsilon_{100}^{II} : \epsilon_{110}^{II}$	$T_{BP-II, c}$
100 : 0	352	{ 0.99±0.03 : 1.00 : 0.37±0.03 0.96±0.03 : 1.00 : 0.31±0.03	91.04 91.19	1.25±0.06 1.56±0.06	2.55±0.20	91.24
80 : 20	478	{ 1.02±0.03 : 1.00 : 0.32±0.03 1.00±0.03 : 1.00 : 0.30±0.03	83.55 83.65	1.33±0.06 1.50±0.06	2.50±0.15	83.68
73 : 27	550	1.05±0.03 : 1.00 : 0.35±0.03	76.40	1.40±0.06	2.50±0.15	76.48
65 : 35	723	1.10±0.04 : 1.00 : 0.28±0.04	77.70	—	—	—
10 : 90	472	0.92±0.03 : 1.00 : 0.33±0.03	66.12	1.37±0.06	2.70±0.15	66.16

Notes: 1) The results for the 73:27 mixture represent a refinement over the results of Ref. 8 in that we have used the oblique-incidence data for the case of heating from the cholesteric phase and averaged over a large number of samples. For all the mixtures at least three better-quality samples were used in the averaging. 2) A comparison of the values of ϵ for the cholesteric and BP-I phases of the various mixtures gave approximately the same results for all: $\epsilon^{CP} : \epsilon_{110}^I = 3.3 \pm 0.3$.

is near the cholesteric–BP-I transition point, the second near the BP-I–BP-II transition. The data for the other mixtures are given for temperatures of the BP-I phase in the middle of its existence interval. The relative values of $\varepsilon_{100}^{\text{II}}$ and $\varepsilon_{110}^{\text{II}}$ for BP-II were determined from the normal-incidence data. The values given in the table correspond to BP-II temperatures near the point of transition to BP-I (here the intensities I_{100} and I_{110} are maximum).

Column 5 gives the values calculated from the ratio of the integrated intensities of the (100) reflections of BP-II, as measured at the temperature indicated in column 7, and the (110) reflections of BP-I, as measured at the temperatures indicated in column 4. It is seen that the values of $\varepsilon_{110}^{\text{I}}$ in the given temperature range fall off appreciably with increasing temperature: by a factor of 1.25 for pure CN and by a factor of 1.13 for the 80:20 mixture. If this is the case, the same can be said of the absolute values of $\varepsilon_{200}^{\text{I}}$ and $\varepsilon_{211}^{\text{I}}$.

In cases where we made a comparative study of the order parameters of the cholesteric and blue phases we used thinner samples, 2–3 μm thick, since at thicknesses of 6 μm the circular dichroism at the selective-reflection peak for the cholesteric phase reached 0.2–0.3, and relation (3) became inapplicable in this case.

Let us now turn to an analysis of the results. It is seen that for all the mixtures the ratio of the components of ε of the two blue phases remains almost constant while the pitch of the cholesteric helix changes by approximately a factor of two; consequently, the structure of the blue phases depends only weakly on the chirality. The weak dependence on the pitch is manifested only in BP-I and amounts to a slight increase in the contribution of the component ε_{110} with decreasing pitch. In addition, the absolute values of ε for different mixtures are also approximately the same, since the integrated intensities of the same reflections in different mixtures (as we have found from measurements not reported here) are approximately equal.

It is also seen that generally speaking the structure of the blue phases also depends on the composition of the mixture—at an almost identical pitch, the data for the 80:20 and 10:90 mixtures are slightly different for the two blue phases.

5. DISCUSSION

As we have seen, the cubic model and the technique used in this study have enabled us to explain all the observed spectral patterns. We were able to identify all the reflections without making additional assumptions—not a single “extra” reflection remains, and the calculated positions agree rather well with the experimental peaks (at any rate if we allow for the dispersion in n).

It is clear from what we have said that, depending on a number of factors, the samples have domain structures with extremely diverse orientations of the blue-phase cells. In a very large number of cases there is assuredly a set of definite preferred discrete orientations. A particularly distinct example is the completely determinate orientation of the cell with respect to the normal to the surface—in both phases this direction coincides with either the [100] or [110] direction.

The set of alternative azimuthal orientations of the BP-II cell in the samples has only two members (Figs. 1f and 1h), with f being the preferred alternative—in this case the sample was single-domain.

The azimuthal orientation of the BP-I cell has a larger number of discrete alternatives. It can also be random, as in the BP-I phase obtained by heating. During the cooling runs the set of discrete orientations shown in Figs. 1b–1e is preferred, with the most common alternatives being c and d . We note that in these orientations of the cell, the direction [110] is normal to the surface, while the directions $[00\bar{2}]$, $[002]$, $[\bar{1}10]$, $[1\bar{1}0]$, $[\bar{1}12]$, $[1\bar{1}2]$, $[\bar{1}\bar{1}2]$, and $[\bar{1}\bar{1}\bar{2}]$, which are perpendicular to it, lie in the plane of the bounding surface, and for each of the alternative orientations listed above, one of these directions must lie either along or across the rubbing direction. This evidently explains why these particular alternatives are preferred.

On the whole, it can be stated that BP-I has a tendency to form a polydomain structure, whereas the BP-II samples, as a rule, are single-domain. The orientation of the blue-phase cells with respect to the bounding surface is governed chiefly by the chemical properties of the latter, which determine the nature of the boundary-layer interactions with the molecules of the liquid crystal. For example, in using purified quartz plates (without a coating), we observed an additional orientation in BP-II, with the [111] direction normal to the surface, while the orientation with normal direction [100] was disadvantageous and was not realized. As we have seen, however, when a coating of polyvinyl alcohol is applied and rubbed, thereby creating a preferred direction in the plane of the substrate, other normal orientations and a series of discrete azimuthal orientations of the blue-phase cells becomes possible.

The second important factor in the orientation of the blue-phase cells is the definite “aftereffect” of the structure of the phase which precedes the transition to the given phase. We have already stressed the difference in the orientations of the cube for the BP-I phase obtained in heating from the cholesteric phase and the phase obtained in cooling from BP-II. When uncoated plates were used we found that the orientation of the BP-I cells upon the transition from the confocal texture of the cholesteric phase was arbitrary; on the other hand, if the transition occurred from the planar texture, then, as in the samples with the coating, the [100] direction in BP-I was clearly fixed along the normal (Fig. 1a), while upon further heating, in BP-II, the [110] direction was aligned with the normal (of course there was no azimuthal orientation in either case).

Finally, if the polyvinyl alcohol substrate had inhomogeneities and defects, the blue phase in the samples could display domains with cell orientations which were atypical for the given conditions (for example, BP-I obtained by cooling from BP-II could have the orientation in Fig. 1a, or BP-II could have that in Fig. 1h), and upon repeated melting and cooling these domains appeared in the same places, i.e., were associated with local features of the surface.

It is extremely important that in all the various orientations of the domain structures, the coexistence of domains

with different cell orientations and even the coexistence of phases lead simply to a superposition of the corresponding circular-dichroism patterns, i.e., do not affect the cell parameters. It is only upon supercooling that the strains mentioned earlier arise. Here the distortion of the cubic cell of BP-I is probably due to the strong influence of the orienting boundary surfaces for relatively thin samples, 10–20 cell dimensions thick. The relative strains are never large—the parameter x in (2) did not exceed 0.05–0.10 in any of the mixtures. In regard to the structure arising after the rearrangement of the BP-I cell upon strong supercooling, we can as yet say only that its cell is also deformed.

The results of this study confirm the conclusion drawn in Ref. 8 that the symmetry space groups of BP-I and BP-II are O^8 and O^2 , respectively. In conclusion we note that the data in Table II permit the assertion that the structures we have described for the two phases are quite universal for all the investigated mixtures—they display only an insignificant dependence on the chirality and chemical composition of the mixture. The available theoretical estimates² of ε are in good agreement with the values obtained for BP-II while for BP-I there is only qualitative agreement with experiment, probably because the (211) harmonic was neglected in Ref. 2. In Ref. 10 the results of computer calculations were presented for the Fourier components of the blue-phase structures. For the groups O^8 and O^2 , at the midrange of the chirality values (on which ε exhibited a weak dependence), the following estimates were obtained: $\varepsilon_{200}^I : \varepsilon_{110}^I : \varepsilon_{211}^I = 1.05 : 1.00 : 0.33$, $\varepsilon_{100}^{II} : \varepsilon_{110}^{II} = 2.55$. It is seen that the agreement of theory and experiment here is very good.

It is still hard to say anything definite about BP-III. Since the values of the circular dichroism here are of the same order of magnitude as in the other phases, there are undoubtedly supermolecular chiral structures present, since the molecular circular dichroism is orders of magnitude smaller. Since the value of the circular dichroism falls off strongly with temperature, one would assume that either there are changes in structure—disordering or a change in pitch—or else there is coexistence of BP-III with the isotropic phase, with the relative content of the latter increasing with temperature. On the other hand, the growth of the cir-

cular dichroism with decreasing wavelength suggests the presence of scattering on large-scale inhomogeneities of the disordering chiral structures.

We are indebted to N. V. Usol'tseva for providing the pure materials and to V. A. Belyakov and V. E. Dmitrienko for a number of helpful discussions.

¹In the non-Soviet literature these phases are called BP-I and BP-II; the third phase, whose nature is unclear, is called BP-III or the fog phase.

²It was for this reason that the surfaces of the cell had to be of high optical quality; the homogeneity of the structure was improved substantially in this case.

³We shall henceforth use the term "reflection," as it is clearer and more descriptive, since the spectral position of a reflection coincides with the directly measured position of a peak in the circular dichroism.

⁴We estimated the dispersion of the refractive index from the data of Ref. 9 for the cholesteric phase; it can be assumed that the differences between the dispersion in the cholesteric and blue phases are not large. An extrapolation to the region $\lambda < 400$ nm shows that the dispersion is not more than $\sim 10\%$ over the region under study.

⁵BP-I supercools very strongly (see below).

⁶They can be detected polarimetrically at the point of the transition from BP-I to BP-II (see Ref. 7).

⁷The cholesteric phase melts here at a temperature of 76.40 °C.

¹S. A. Brazovskii and S. G. Dmitriev, *Zh. Eksp. Teor. Fiz.* **69**, 979 (1975) [*Sov. Phys. JETP* **42**, 497 (1975)].

²H. Grebel, R. Hornreich, and S. Shtrikman, *Phys. Rev. A* **28**, 1114 (1983).

³V. A. Belyakov, V. E. Dmitrienko, and S. M. Osadchii, *Zh. Eksp. Teor. Fiz.* **83**, 585 (1982) [*Sov. Phys. JETP* **56**, 322 (1982)].

⁴H. Stegemeyer and K. Bergmann, in: *Liquid Crystals of One- and Two-Dimensional Order* (ed. by W. Helfrich and G. Heppke), Springer-Verlag, Berlin (1980), p. 161.

⁵S. Meiboom and M. Sammon, *Phys. Rev. Lett.* **44**, 882 (1980); *Phys. Rev. A* **24**, 468 (1981).

⁶D. L. Johnson, J. H. Flack, and P. P. Crooker, *Phys. Rev. Lett.* **45**, 641 (1980); J. H. Flack, P. P. Crooker, and R. Svoboda, *Phys. Rev. A* **26**, 723 (1982).

⁷M. Marcus, *Phys. Rev. A* **25**, 2272, 2276 (1982).

⁸V. A. Kizel' and V. V. Prokhorov, *Pis'ma Zh. Eksp. Teor. Fiz.* **38**, 283 (1983) [*JETP Lett.* **38**, 337 (1983)].

⁹B. Boettcher and G. Graber, *Mol. Cryst. Liq. Cryst.* **14**, 1 (1971).

¹⁰V. A. Belyakov, V. E. Dmitrienko, and S. M. Osadchii, *Proc. Fifth Conf. of Socialist Countries on Liquid Crystals* [in Russian], Odessa (1983), Vol. I., Part 2, p. 14.

¹¹V. A. Belyakov and A. S. Sonin, *Optika Kholestericheskikh Zhidkikh Kristallov* [Optics of Cholesteric Liquid Crystals], Nauka, Moscow (1982), Sec. 8.4, p. 313.

Translated by Steve Torstveit